



Histopathological investigation of four populations of abalone (*Haliotis iris*) exhibiting divergent growth performance

Joanna S. Copedo^{a,b,*}, Stephen C. Webb^a, Norman L.C. Ragg^a, Leonie Venter^b,
Andrea C. Alfaro^b

^a Cawthron Institute, Nelson 7042, New Zealand

^b Aquaculture Biotechnology Research Group, Department of Environmental Sciences, School of Science, Auckland University of Technology, Private Bag 92006, Auckland 1142, New Zealand

ARTICLE INFO

Keywords:

Abalone
Food limitation
Haliotis iris
Histopathology
Kidney crystals
Sand incursion

ABSTRACT

The black-foot abalone (pāua), *Haliotis iris*, is a unique and valuable species to New Zealand with cultural importance for Māori. Abalone are marine gastropods that can display a high level of phenotypic variation, including slow-growing or 'stunted' variants. This investigation focused on identifying factors that are associated with growth performance, with particular interest in the slow-growing variants. Tissue alterations in *H. iris* were examined using histopathological techniques, in relation to growth performance, contrasting populations classified by commercial harvesters as 'stunted' (i.e., slow-growing) and 'non-stunted' (i.e., fast-growing) from four sites around the Chatham Islands (New Zealand). Ten adults and 10 sub-adults were collected from each of the four sites and prepared for histological assessment of condition, tissue alterations, presence of food and presence of parasites. The gut epithelium connective tissue, digestive gland, gill lamellae and right kidney tissues all displayed signs of structural differences between the slow-growing and fast-growing populations. Overall, several factors appear to be correlated to growth performance. The individuals from slow-growing populations were observed to have more degraded macroalgal fragments in the midgut, increased numbers of ceroid granules in multiple tissues, as well as increased prevalence of birefringent mineral crystals and haplosporidian-like parasites in the right kidney. The histopathological approaches presented here complement anecdotal field observations of reduced seaweed availability and increased sand incursion at slow-growing sites, while providing an insight into the health of individual abalone and sub-populations. The approaches described here will ultimately help elucidate the drivers behind variable growth performance which, in turn, supports fisheries management decisions and future surveillance programs.

1. Introduction

The New Zealand (NZ) black-foot abalone, *Haliotis iris* (Gmelin, 1791), locally known as pāua, is one of three haliotid species commonly found around the New Zealand rocky shores at depths of approximately 15 m, typically between 0.5 and 7 m (Poore, 1973; McShane et al., 1994). Since the early 1990s, *H. iris* has been gaining a foothold as a key aquaculture species and is still an important wild fisheries species for New Zealand.

Abalone have a mostly sedentary lifestyle and feed on various attached and drifting seaweed (Poore, 1972; Allen et al., 2006). Due to this limited mobility, they are exposed to several environmental stresses and their diet is dependent on local supply and hydrographic processes,

such as tidal currents (Poore, 1972; Allen et al., 2006; Laferriere, 2016; Morash and Alter, 2016). They occupy varied habitats that can be considered optimal or sub-optimal. Correspondingly, *H. iris* can show a large variation in morphology and growth phenotypes (Saunders, Mayfield and Hogg, 2008; Saunders, Connell and Mayfield, 2009), which may reflect the presence of slow-growing or 'stunted' populations (Naylor and Andrew, 2004; Naylor et al., 2007; Saunders, Mayfield and Hogg, 2008; Saunders, Mayfield and Hogg, 2009; Laferriere, 2016).

Stunted populations show chronic slow growth, which results in reduced size-at-age when compared with 'normal' growing populations (Wells and Mulvay, 1995; Saunders, Mayfield and Hogg, 2008). Growth suppression can be most apparent in the shell profile, or the shell length: height ratio, resulting in relatively high and wide individuals compared

* Corresponding author at: Cawthron Institute, Nelson 7042, New Zealand.
E-mail address: Joanna.copedo@cawthron.org.nz (J.S. Copedo).

to their non-stunted conspecifics (Saunders, Mayfield and Hogg, 2009). The changes in shell morphology are likely to reflect diminished longitudinal calcite layer growth, while accretion of the inner nacreous layer continues. There are specific areas along the North and South Islands of New Zealand where abalone populations do not reach the minimum legal fishing size limit of 125 mm shell length; these are generically referred to as ‘stunted’ populations (McShane et al. 1994c, Naylor et al., 2006). This phenomenon has been observed in a number of mollusc species, including mussels (e.g., *Mytilus galloprovincialis*, Hine, 1997), oysters (e.g., *Crassostrea gigas*, Hine, 1997; Kang et al., 2010), the land snail, *Patera appressa* (Martin and Bergey, 2013), the abalone, *Haliotis rubra* (Saunders, Mayfield and Hogg, 2008) and *H. iris* (McShane and Naylor, 1995; Saunders, Connell and Mayfield, 2009), as a result of complex environmental interactions. ‘Stunted’ abalone occur around New Zealand and can typically be found in sheltered areas protected from wave action, which typically have low flow, reduced complexity in terms of substrate topography (Laferriere, 2016), and low seaweed abundance (Saunders, Connell and Mayfield, 2009). In sheltered areas with low wave action, sediment will also accumulate (Schiel et al., 2006). Non-stunted *H. iris* can generally be found in areas with higher wave action, increased food and topographic complexity, where drift seaweed may collect (Saunders, Connell and Mayfield, 2009; Laferriere, 2016).

The complex relationship of extrinsic and intrinsic drivers affects the growth rate of marine molluscs (Ren et al., 2019; Saulsbury et al., 2019). The range of these factors is diverse and not only includes the quality and the quantity of food, but also water quality parameters, such as temperature, water velocity, salinity, and pH (Diggles et al., 2002; Searle, Roberts and Lokman, 2006; Bergström and Lindgarth, 2016), as well as reproductive state, immune response and parasite association (Diggles et al., 2002; Morash and Alter, 2016; Wu, Kaiser and Jones, 2018). Variations between these factors are likely to result in morphometric variation within a species (Ren et al., 2019). The two most well-studied predictors of growth rate are food availability and temperature (Saulsbury et al., 2019). Sedentary marine invertebrates have been reported to display high variations in morphology associated with responses to environmental stresses (Trussell, 1996; Steffani and Branch, 2003; Saunders, Connell and Mayfield, 2009). Coastal ecosystems are often highly impacted by increasing environmental stresses underpinned by climate change (Halpern et al., 2008; Lima and Wethey, 2012). Global sea surface temperature trajectories indicate that most coastlines are experiencing less frequent cold days and a significant increase in marine heatwaves (Halpern et al., 2008; Lima and Wethey, 2012). These environmental stresses not only drive habitat alterations, but may result in episodes of mass mortalities of invertebrates and could have enduring negative impacts on populations (Soon and Ransangan, 2019).

The Chatham Islands (43°53'S, 176°31'W) lie in an oceanic convergence zone, influenced by both colder southern water and warmer northern water, having predominantly a temperate climate (Wilcox, 2007). The islands (commercial area PAU4) support the largest abalone fishery in New Zealand. Both ‘stunted’ (slow growing) and ‘non-stunted’ (fast-growing) populations around the Island within the commercial fishery have been observed by divers and fisheries managers and there is a growing concern for the future performance of local *H. iris* populations. Additionally, the reduced growth to minimum legal catch size results in light catches and dense population numbers. Therefore, it is crucial to understand the causes of divergent growth performance in wild populations of *H. iris*, especially with regards to the complex abalone-environment interactions and potential role of pathogens. In the current study, histopathological tools were used to compare tissue alterations on four populations of abalone to investigate tissue-level responses and potential ecological causes of the observed variation in growth performance.

2. Methods

2.1. Sampling locations and animal collection

The Chatham Islands are located approximately 800 km east of New Zealand’s South Island. Four geographically distinct sites were selected based on the growth performance differences among resident abalone populations established by monitoring within the commercial fishery (Fig. 1).

Sites were characterised based on direct observations, growth performance and commercial abalone harvest performance (historic data and personal communications: Pāua Industry Council Ltd).

Site 1 (Ascots) supports an abalone population of ‘fast-growing’ individuals that readily reach the legal fishing size of 125 mm and are therefore fished more often. The site was characterised as having spaces of bare rock and sand with a high density and diversity of seaweed, with dominant resident species, including green (e.g., *Ulva lactuca*, *Chaetomorpha coliformis*), brown (e.g., *Zonaria turneriana*, *Cystophora scalaris*) and red (e.g., *Gigartina clavulatum*) macrophytes, with an abundant supply of mixed drift algae (unpublished observations, March 2020).

Site 2 (Owenga harbour) had a dense abalone population of ‘stunted’ individuals, with very few reaching the legal catch size. The habitat was characterised as having extensive bare rock and sandy areas with low seaweed diversity and density, the dominant species being the chlorophyte *Ulva lactuca* and phaeophytes (e.g., *Cystophora scalaris*).

Site 3 (Durham) was considered to have ‘stunted’ growth performance. The site had areas of bare rock and gravel. Seaweed density and diversity was intermediary between sites 1 and 2, dominated by phaeophytes (e.g., *Cystophora scalaris*) and chlorophytes (e.g., *Ulva lactuca*, drift and attached).

Site 4 (Wharekauri harbour) was considered ‘fast-growing’. The site was characterised by extensive bare rock. The dominant seaweed species being the brown kelp *Durvillaea chathamensis* with representatives of other phaeophytes (e.g., *Cystophora scalaris*) and chlorophytes (e.g., *Ulva lactuca*).

A total of 10 adults (pāua identified to be > 110 mm, >250 g live mass) and 10 Sub-adults (Pāua identified to be < 110 mm, <250 g) were randomly collected by divers from each of the four sites in sets of 10 over 3 days for surveillance. Individuals were measured to the nearest 0.1 mm for shell length (SL), and weighed to the nearest 0.1 g (W), followed by retrospective measurements of shell width (SW), shell height (SH)

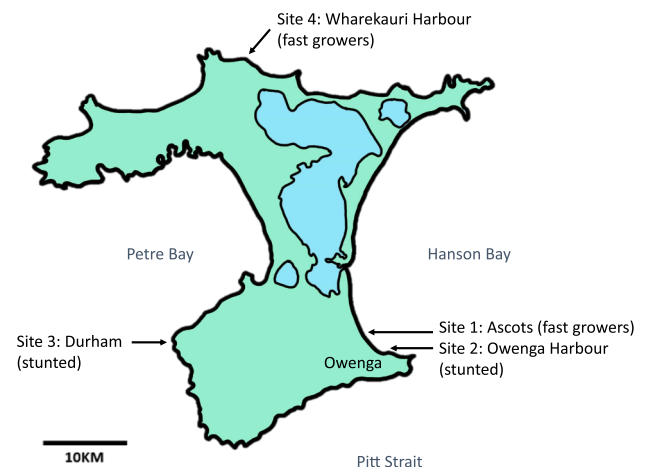


Fig. 1. Generalised map of Chatham Island (43°52'49.7" S 176°32'02.6" W) depicting the four selected ‘stunted’ or ‘fast-growing’ sites selected for sampling. Site 1: Ascots (44°00'56" S 176°23'12" W); Site 2: Owenga harbour (44°01'28" S 176°21'56" W); Site 3: Durham (44°00'24" S 176°40'54" W) and Site 4: Wharekauri Harbour (43°42'18" S 176°35'04" W)..

and calculation of the SL: SH ratio before sampling and histological preparation. Sampling per individual occurred within 15 min. Additionally, the sex of each individual pāua was recorded and confirmed using histological techniques, and both percent population reproductively active and the F:M sex ratio were reported.

2.2. Histopathological preparation

Tissue was removed from the shell to expose the organs and the viscera dissected and sectioned as shown in Fig. 2. The sectioned samples (midgut, digestive gland, left and right gill, left and right kidney) were carefully placed into histological cassettes and fixed in a 4 % formalin solution (1:9 v/v, 37 % Formaldehyde:0.35 µm filtered seawater) for 48 h before being transferred into 70 % ethanol for processing (Howard, 2004). Samples were dehydrated, cleared, and embedded in paraffin wax, sectioned (3–5 µm) using a microtome and stained using routine hematoxylin and eosin (H&E).

A range of tissues were examined under a compound light microscope (Olympus BX40) at magnifications from x40 to x1000, including midgut, digestive gland, gills, gonad, kidneys, hypobranchial gland, nervous tissue, and muscle. Semi-quantitative scales were devised and used to grade deviations from normality for the midgut, digestive gland, gill, and right kidney (see below sections 2.2.1. to 2.2.4.).

Initial surveillance revealed tissue anomalies between the 'stunted' and fast-growing populations. The anomalies were observed in the algae condition within the stomach/crop, digestive gland, gill, and right kidney and these tissues were therefore targeted for this investigation.

2.2.1. Food scoring and ceroid analysis

Gut contents were scored semi-quantitatively across the samples of the posterior section of midgut. Only food items that were clearly inside the crop/stomach region were scored using a subjective criterion on a grade scale from 1 to 5. Grade 1 = 100 % Fresh, Grade 2 = 75 % Fresh: 25 % Old, Grade 3 = 50 % Fresh: 50 % Old, Grade 4 = 25 % Fresh: 75 % Old, Grade 5 = 100 % Old. 'Fresh' algae fragments were large and retained cellular structure (Fig. 3a), 'Old' Algae describes a mixture of fine debris and degraded algae cellular structure (Fig. 3b).

The presence of ceroid granules (a brown oxidised lipid material) was scored semi-quantitatively based on level of accumulation within the interstitial tissue of the gastrointestinal tract, digestive gland, and kidney. Histopathological alterations (i.e. ceroid granules) were categorised as described by Costa et al. (2013) and Muznebin, Alfaro and

Webb (2022) with minor modifications. In brief, ceroid granules were categorised by level of severity 0: None observed, 1: Mild (light or occasional scattering), 2: Moderate (light scattering with occasional focal dense patches) and 3: High, (dense, diffuse, and frequent patches) (Fig. 4).

2.2.2. Digestive gland scoring

Criteria were developed to semi-quantitatively score the severity of the alteration in the digestive gland tubules, refining a general alteration scoring system proposed by Knowles et al. (2014), Fraga et al. (2022) and Perez-cebrecos et al. (2022):

Criterion 1: The proportion of tubules (coverage) with separation of digestive epithelium from the basement membrane. Score of 0 = No spaces seen (Fig. 5a), Score of 1 = Less than 25 % of epithelial cells had spaces, Score of 2 = Between 25 and 50 %, Score of 3 = Between 50 and 75 %, Score of 4 = More than 75 % were shown to have spaces.

Criterion 2: A gauge of the extent of separation on each tubule (extent): Score of 0 = No spaces, Score of 1 = Less than 25 % of the tubule is retracting, Score of 2 = Between 25 and 50 % tubule retraction, Score of 3 = Between 50 and 75 % tubule retraction, Score of 4 = More than 75 % of the tubule was shown to have retracted away from connective tissue (Fig. 5b).

Criterion 3: The quality of the digestive tubule (termed 'DG quality') was determined by the following factors: 1. alteration of the basophilic pyramidal cells (Shumway and Parsons, 2011; Cuevas et al., 2015), as well as 2. the staining affinity of these cells, 3. lumen shape, 4. increased number of ceroid granules within the tubule wall, 5. level of hemocytes near connective tissue and 6. presence of oedema in interstitial spaces. A score of 0: apparent normality (Fig. 5a), 1: minor alterations to tissue architecture, 2: 1/2 of the tissue architecture impacted and/or displayed 2–4 of the 6 factors above, 3: 3/4 of tissue affected and 4 to 6 of the factors above observed, 4: whole tissue structure affected and 4–6 of the factors observed was applied (Fig. 5).

2.2.3. Gill

The gills were screened for pathogens and abnormalities. The number of ciliates per frame was counted to characterise the alterations observed in gill tissue. An 1857 × 3308 µm frame at 40x magnification was selected as the optimal area to include the full lamella length (Fig. 6). The counts were then converted to a standardised value per 1 mm² of lamella cross-sectional area. This approach represents a refinement of standard surveying performed at 200x magnification. To

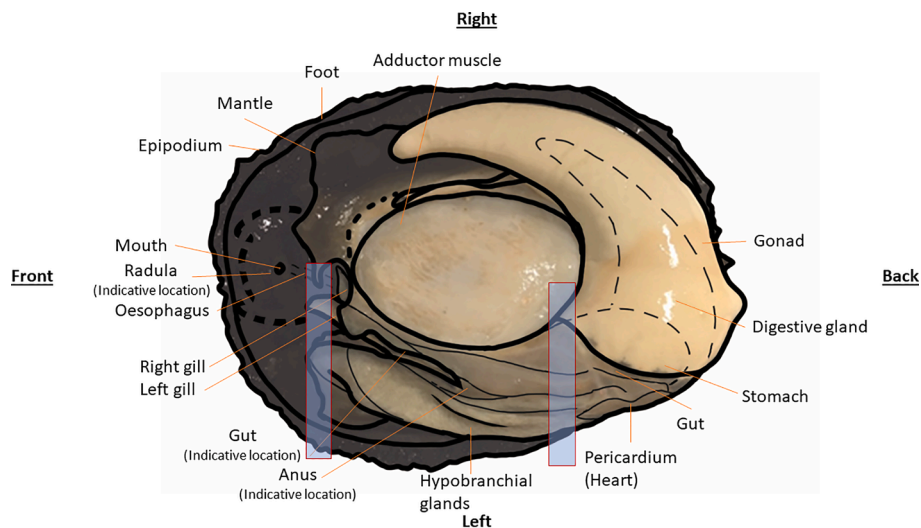


Fig. 2. General anatomy depiction of New Zealand abalone (*Haliotis iris*). Rectangular windows show approximate location of the histology sections, which were chosen to maximise chances of acquiring all tissue types, including midgut, digestive gland, left and right gill, gonad, left and right kidney, hypobranchial gland, nervous tissue, and muscle.

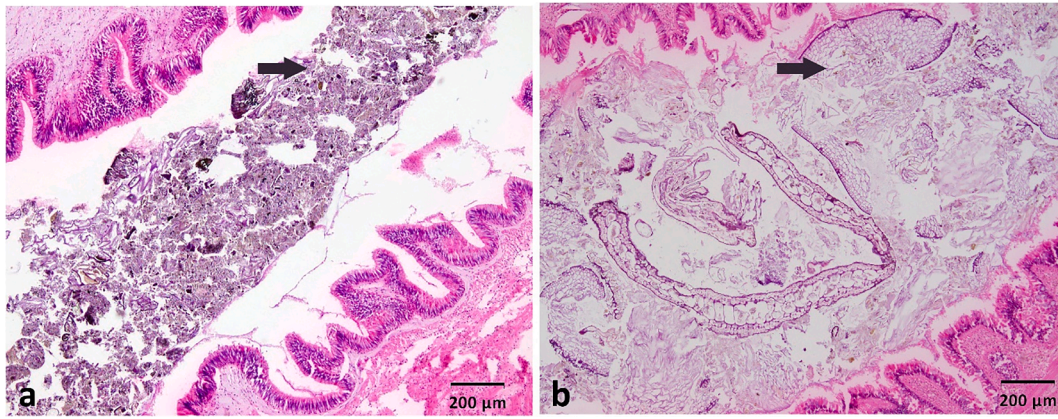


Fig. 3. Photomicrographs of the crop/stomach region of *H. iris*. a) Grade 5: 'Old', where algal material has broken down to fine particles of grey-coloured debris (arrow). b) Grade 1: 'Fresh', where structure of the algae is still largely intact and cells still visible (arrow). Grades 2 to 4 (not shown here) represent intermediate conditions as defined in the text in section 2.2.1.

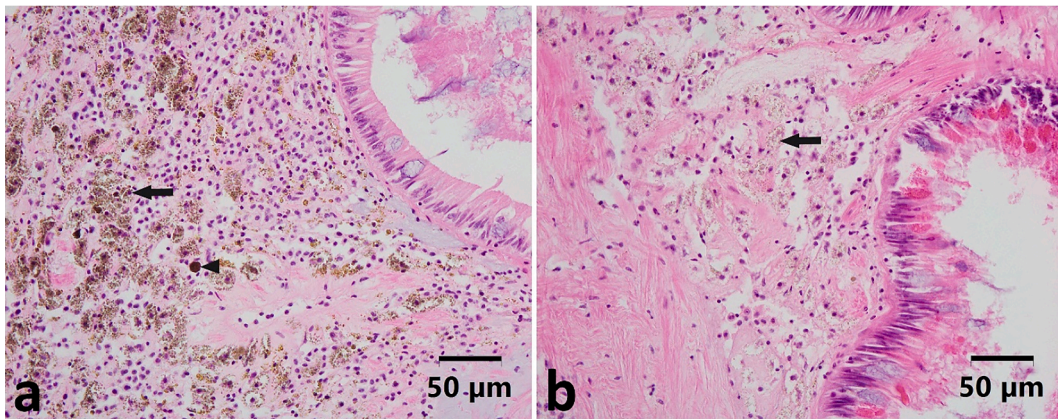


Fig. 4. Mid-gut sub-epithelium from a) slow-growing individual (site 2: Owenga harbour) showing the high level (score 3) of ceroid material presence, and b) fast-growing individual (site 1: Ascots) showing minimal ceroid material (score 1). Examples of fine ceroid granules (Arrow) and ceroid aggregate (Arrowhead) are marked.

validate the use of the larger frame size, five individuals were randomly selected for further analysis. Ciliates in five random sections of gill at 200x were counted and averaged. It was observed that the average of 5 smaller frames lead to greater variation in the estimated number per mm^2 due to non-homogenous focal presence of the ciliates, indicating that a single large frame introduced less risk of bias.

2.2.4. Right kidney

Presence/absence of haplosporidian-like parasites and kidney crystals were recorded and expressed as percentage prevalence for each sample population. Initial detection of the kidney crystals was performed using cross polarisation of the light source to highlight birefringent properties. For photograph imaging only one of the polarising filters was required. This application allowed for the clearer detection of the birefringent properties of the kidney crystals. By further reducing the camera exposure to $-2/3$ this balanced the brightness of the reflective light and facilitated the detection of very small crystals that were not otherwise noticeable at the magnifications applied here.

2.3. Statistical analyses

Data were checked for normality and heterogeneity of variance using the Shapiro-Wilks and Levene's tests, respectively. Site and life stage were used as factors in the models used. The majority of the semi-quantitative data including parameters of the midgut and digestive gland data were treated as non-parametric. Ordinal Logistic Regression

(OLR) models and linear models were used to detect differences, performed using the MASS package (Venables and Ripley, 2002). A GLM was used to analyse the ciliate numbers as well as morphometric data. The ciliate data was log-transformed to meet the assumption of homogeneity of variance. Post-hoc pairwise analysis was performed using the package emmeans (Lenth, 2021). Followed by p value adjustment using tukey method to avoid cumulative type I error. For prevalence data (i.e., presence/ absence) of kidney crystals or haplosporidian-like parasites, general linear models (GLM) using binomial data was used to detect differences. As a result of the "perfect" separation between responses, a ridge penalizer was used to add a 'ridge prior' to the estimates in order to increase sensibility of the parameter estimates (Cule and Frankowski, 2021). Un-transformed data were used for the graphs. R version 4.0.3 (R Core Team, 2021) was used for statistical analysis.

3. Results

There were statistically significant interactive effects between site and life stage in weight ($\chi^2_{(3)} = 94.16, p = <0.001$) (Table S1), shell length ($\chi^2_{(3)} = 39.55, p = <0.001$) (Table S2), shell width ($\chi^2_{(3)} = 9.43, p = 0.024$) (Table S3), shell height ($\chi^2_{(3)} = 10.81, p = 0.013$) (Table S4), and no statistical interaction effects between site and life stage on shell length: shell height ratio ($\chi^2_{(3)} = 6.18, p = 0.103$). However, for the shell length: shell height ratio both site and life stage were individually affected (Site: $\chi^2_{(3)} = 18.66, p = <0.001$, and life stage: $\chi^2_{(1)} = 14.09, p = <0.001$). Ascotts and Durham had lower height to shell ratio when

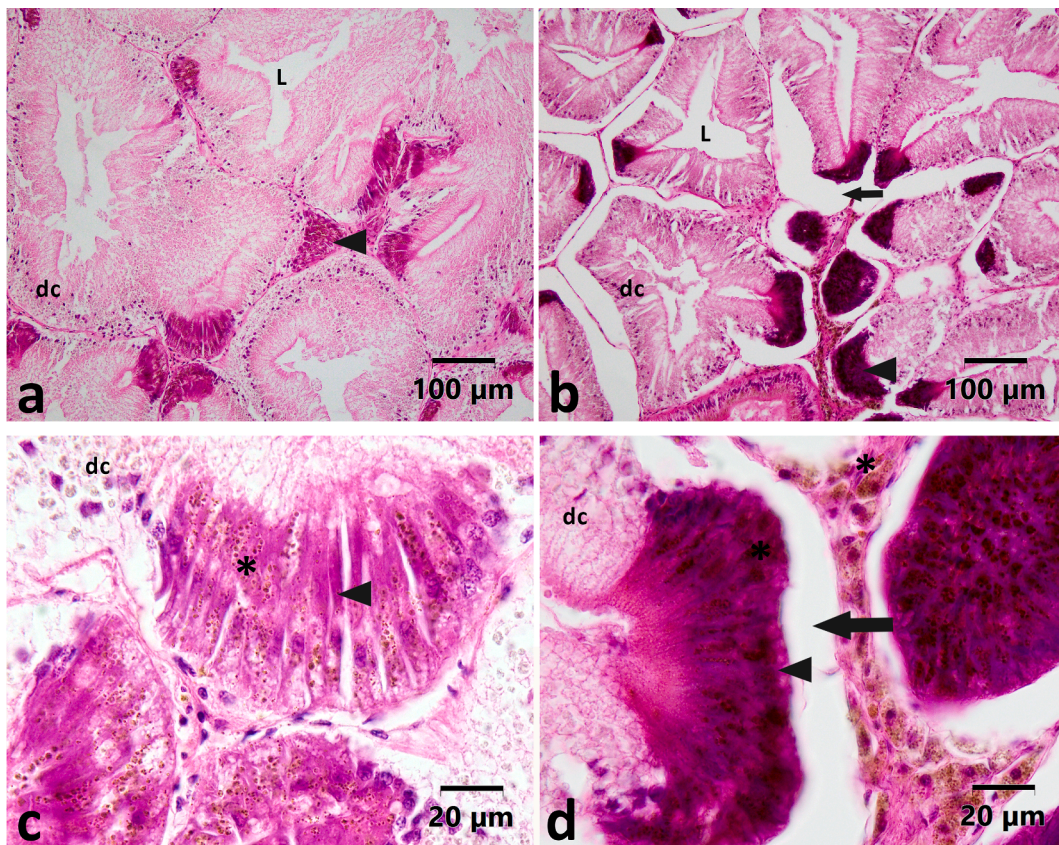


Fig. 5. Scoring criteria to quantify the severity of the alterations in the digestive gland tubules of *Haliotis iris*. a) Normal digestive gland tissue whereby none of the digestive tubules are showing signs of gapping and all are tightly packed (Score 0). b) Digestive gland tissue showing signs of gapping away from basement membrane (Score 3) and poor-quality tubules (DG quality score 3) displaying changes to basophilic cells and increased staining affinity, developing space in interstitial space and increased hemocytes (arrow). Digestive tubule lumen (L), digestive cells (dc) and basophilic cells (arrowhead) of the digestive tubule epithelial layer are indicated. c) Zoom of digestive gland (a) showing connection of the epithelium to the basement membrane. Section shows pink/purple-toned basophilic cells (arrowhead), a light scattering of ceroid granules (star) in basophilic cells. d) Zoom of image b showing separation of epithelium from the basement membrane creating a void (arrow), compression of the basophilic pyramidal cells and an increase in ceroid material in both the basophilic cells and interstitial tissue. (For interpretation of the references to colour in this figure legend, the reader is referred to the web version of this article.)

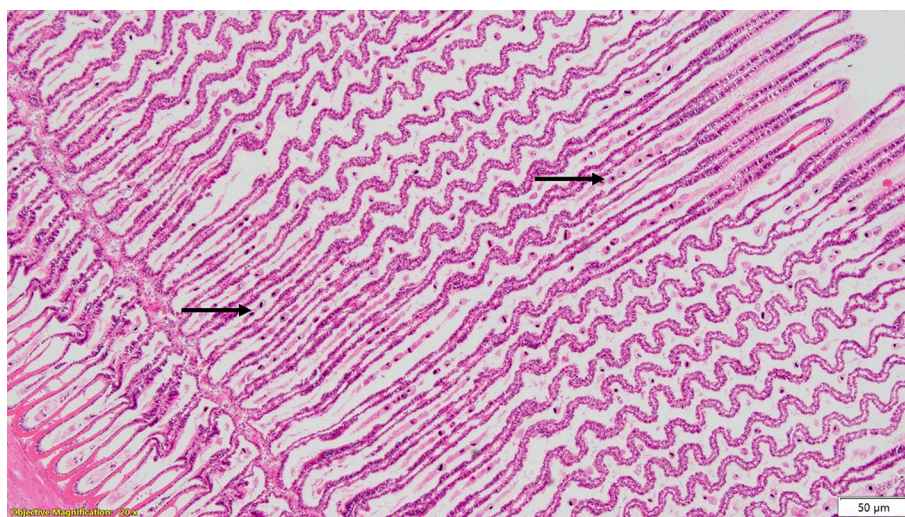


Fig. 6. Example photomicrograph (Frame size: 1857 × 3308 μm) of *H. iris* gill, *Sphenophyra*-like ciliates with dense nuclei are shown (black arrows) between the gill filaments.

Table 1

Morphometric and physiological data whereby size range is the min and max shell length. Additional values report the mean ± StdDev (Sd). Weight in g (W), Shell length in mm (SL), Shell width in mm (SW), Shell height in mm (SH) shell length to shell height ratio (SL:SH), Percent population reproductively active (% RA) and the female: male sex ratio (F:M).

		Size	W (±Sd)	SL (±Sd)	SW (±Sd)	SH (±Sd)	SL:SH (±Sd)	% RA	F:M
Adult	Ascots	121–138	440 ± 41	131 ± 4.4	99 ± 4	46 ± 2.6	2.9 ± 0.2	100	0.3
	Owenga	110–122	228 ± 25	117 ± 4.0	89 ± 5.9	37 ± 3.6	3.2 ± 0.3	100	0.7
	Durham	126–147	461 ± 36	131 ± 5.9	97 ± 5.9	45 ± 2.8	2.9 ± 0.3	100	4
	Wharekauri	136–149	526 ± 62	143 ± 5.2	107 ± 7.6	40 ± 3.5	3.6 ± 0.4	100	2.3
Sub-adult	Ascots	69–93	77 ± 20	80 ± 6.3	61 ± 4.2	23 ± 2.3	3.5 ± 0.3	50	0.3
	Owenga	78–88	92 ± 14	85 ± 3.1	60 ± 4.5	21 ± 2.5	4.2 ± 0.6	50	4
	Durham	77–101	120 ± 42	90 ± 7.4	65 ± 6	26 ± 4.8	3.6 ± 0.4	60	0.5
	Wharekauri	82–102	118 ± 28	92 ± 7.0	69 ± 3.7	23 ± 1.6	4.0 ± 0.3	50	1.5

compared to Owenga and Wharekauri ($p < 0.0028$ and $p < 0.001$, $p < 0.0091$ and $p < 0.001$, respectively) (Table 1).

3.1. Midgut: Algal quality scoring

There were significant site specific differences whereby the faster growing sites appeared to have fresher (more intact) food in the gut when compared to the ‘stunted’ sites ($\chi^2 = 50.56$, $p < 0.001$) (Fig. 7) (Table S5). There was no significant site and life stage interaction ($\chi^2_{(3)} = 1.08$, $p = 0.78$); Additionally, sand particles were observed in the wax blocks of some individuals (Fig. 8).

3.2. Tissue anomalies

There were no significant site and life stage interactions in the number of ceroid granules (ceroid score) observed in gut epithelium connective tissue ($\chi^2_{(3)} = 0$, $p = 1.0$) however there was a site-specific difference ($\chi^2_{(3)} = 51.56$, $p < 0.001$) (Table 2) (Table S6). It was also noted that the ceroid levels within the connective tissue was also perceptibly higher than in individuals collected from site 2. There was no site and life stage interactions in the proportion of digestive gland tubules detaching (coverage) from the basement membrane creating voids ($\chi^2_{(3)} = 3.69$, $p = 0.3$). There was however a site-specific difference ($\chi^2_{(3)} = 9.93$, $p = 0.019$) (Table S7). There was a significant site and life stage interaction in the average extent of the void around each of the tubules ($\chi^2_{(3)} = 9.05$, $p = 0.029$) (Table S8). Whereby the adults at site 1 had lower scores when compared with the adults at site 2 and site 3

($p = 0.0006$ and $p = 0.04$ respectively) (Table 2). There were no differences in the digestive gland quality between the sites ($\chi^2_{(3)} = 0.697$, $p = 0.87$). There was a significant site and life stage interaction in the number of ceroid granules within the digestive gland connective tissues ($\chi^2_{(3)} = 20.72$, $p < 0.001$) (Table 2) (Table S9).

3.3. Gill

Ciliates (Protozoa, Ciliophora) were commonly found between the lamellae of the gill. The ciliates were identified to be ectocommensal *Sphenophyra*-like ciliates (Diggles and Oliver, 2005; Muznebin, Alfaro and Webb, 2021) by the macronucleus, which is densely basophilic. Ciliates were detected at all sites. There was no interaction between site and life stage ($f_{(68, 3)} = 1.3$, $p = 0.28$) but a site specific difference ($F_{(68, 3)} = 3.98$, $p = 0.011$) (Table S10) (Fig. 9).

3.4. Right kidney

Kidney crystals of a crystalline structure were found to occur with a higher prevalence at site 2 ($t = 2.852$, $p = 0.004$) and site 3 ($t = 3.830$, $p < 0.001$) when compared to the site 1 (Fig. 10). There was a significant difference between adults and sub-adults in the prevalence of kidney crystals ($t = -2.977$, $p = 0.002$). The larger crystals reaching between 50–60 μm . (Fig. 11a–c).

A haplosporidian-like parasite was observed in the right kidney of *H. iris* (Fig. 12) collected from all four sites. There was a population prevalence of 60 % in the adults at site 2 and 4 and only 20 % and 10 % at site 1 and site 4, respectively. Additionally, the sub-adults at site 2 also had a population prevalence of 60 % for haplosporidian-like parasite detection (Fig. 10); however, the low sensitivity of the binomial GLM analysis required for this data format failed to detect significant differences.

4. Discussion

Attributed site-specific growth performance appears to be correlated with alterations found in the midgut (algae structure), digestive glands, and right kidney of *H. iris*. From the histopathological investigations, there are several factors that could potentially affect the growth of the abalone: 1) The differences in macroalgal integrity (‘food score’) in the stomach/crop lumen may reflect variability in the quality, access to food, and digestibility of food indicating a potential nutritional effect. 2) The appearance of sediment particles and the relationship to algae food particles could indicate reduced nutrition, as well as consumption and introduction of excess toxins or minerals. 3) The ceroid material in the connective tissue, as well as the crystals found in the right kidney suggests that there may be either site-specific water quality issues, prior pathogen incursion or advanced age. 4) The appearance of kidney crystals and a haplosporidian-like parasite could be impacting the performance of the kidney.

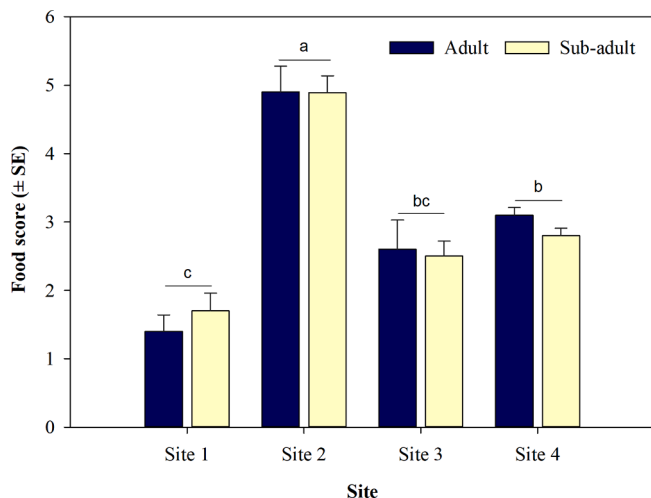


Fig. 7. Food score (Mean ± SE) 1 being 100 % Fresh (intact) food visible and 5 being 100 % old (degraded/digested) food (Adults: site 1. Ascots n = 9, site 2. Owenga n = 9, site 3. Durham n = 7, site 4. Wharekauri n = 10; Sub-adults: site 1. Ascots n = 10, site 2. Owenga n = 9, site 3. Durham n = 10, site 4. Wharekauri n = 10). Significant differences ($p < 0.05$) among groups are shown with lower case letters above bars.

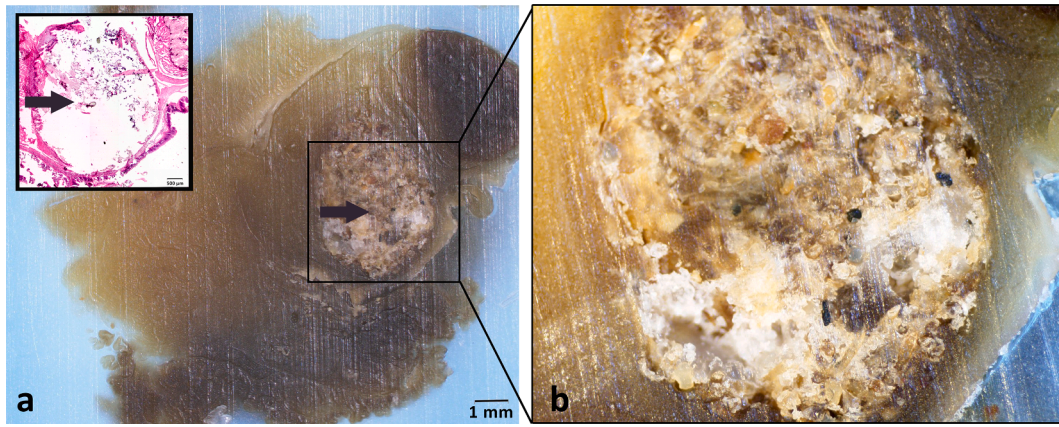


Fig. 8. Histology wax block of an example individual with “older” food and almost empty mid-gut tract. a) histology block sample photographed at ~5x magnification (dissection microscope), indicating a gut lumen filled with sediment (arrow); inset is the corresponding histology slide stained with H&E. b) Enlarged image of gut tract showing sediment particles.

Table 2

Summary of semi-quantitative tissue assessments. Ceroid material in the GE (gut sub-epithelium) reflects the relative quantity (0 – 3) of ceroid material in the connective tissue adjacent to the gut epithelium. ‘Coverage’ (criterion 1) provides an indication of the proportion of digestive tubules showing detachment (score 1 – 4 corresponding to 0 – 100% occurrence), while ‘extent’ (criterion 2) considers the average extent to which tubules have detached (0 – 4 corresponds to no detachment and whole tubule has detached, respectively). The subjective ‘DG quality’ (criterion 3) classifies the overall quality of the tubules. Ceroid score in DG reflects the relative quantity in the interstitial spaces.

		Adults				Sub-adults			
		Site 1. Ascots	Site 2. Owenga	Site 3. Durham	Site 4. Wharekauri	Site 1. Ascots	Site 2. Owenga	Site 3. Durham	Site 4. Wharekauri
Mid-gut epithelium	Ceroid score	1.0 ± 0.0	3.0 ± 0.0	2.7 ± 0.5	1.0 ± 0.0	1.0 ± 0.0	1.4 ± 0.5	1.0 ± 0.0	1.0 ± 0.5
Digestive gland	Coverage	0.8 ± 0.4	2.2 ± 0.7	2 ± 0.9	1.6 ± 1.8	1.3 ± 1.2	1.4 ± 1.1	1.5 ± 0.7	1.0 ± 0.7
	Extent	0.8 ± 0.4	2.6 ± 0.7	2 ± 0.8	1.6 ± 1.5	1.1 ± 0.7	1.2 ± 0.8	1.5 ± 0.8	0.9 ± 0.6
	DG quality	1.5 ± 0.8	2.75 ± 1.3	2.5 ± 0.9	2.8 ± 1.0	1.4 ± 1.0	1.5 ± 1.2	2 ± 0.7	2.0 ± 0.8
	Ceroid score	2.0 ± 0.8	3 ± 0.0	1.8 ± 0.9	1 ± 0.0	1.9 ± 0.6	2.1 ± 0.6	1.8 ± 0.5	1.6 ± 0.5

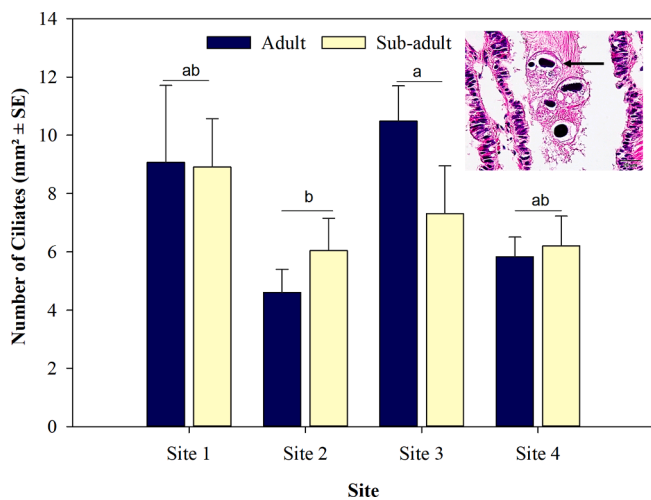


Fig. 9. Number of ciliates per 1 mm² of abalone gill transverse section (Mean ± SE) from four sites around the Chatham Island (Adults: site 1. Ascots n = 10, site 2. Owenga n = 9, site 3. Durham n = 10, site 4. Wharekauri n = 10; Sub-adults: site 1. Ascots n = 10, site 2. Owenga n = 10, site 3. Durham n = 8, site 4. Wharekauri n = 9). Inset: Enlarged image of a group of 4 ciliates (Arrow).

4.1. Nutrition

Abalone from the Ascots and Owenga sites were found to have differences in the integrity of macroalgal food found in the stomach/crop

region. This suggests that either food supply was limiting, and therefore old food tended to persist in the gut, or the food available was tougher and less digestible and therefore remained in the gut for a longer period of time (Day and Cook, 1995; Britz, Hecht and Knauer, 1996). Additionally, they were preferentially selecting algae depending on availability. At site 1 (Ascots), *H. iris* have access to a diverse assemblage of green, red, and brown seaweed types (unpublished observations) and do not appear to be food limited. Conversely, the macroalgal assemblage available to the ‘stunted’ population at site 2 (Owenga) is limited to approximately 8 species of seaweed. Abalone growth is known to improve when individuals feed on a variety of macroalgal species compared to single species (Stuart and Brown, 1994; Mai, Mercer and Donlon, 1995; Viera et al., 2011), particularly if that species is of limited nutritional value. The decrease in topographic complexity at site 2 is also likely to reduce the availability of drift seaweed, further limiting food availability. Poore (1972) correspondingly found that a limited supply of drift weed led to slower abalone growth. Additionally, phaeophytes, which were common at site 2, contain phlorotannin’s which can potentially reduce digestibility and damage the intestinal tract walls (Day and Cook, 1995). No anomalies in the intestinal tract, other than algal quality, were initially observed at the start of this investigation. Therefore, it is likely that the potential consumption of phaeophytes that contain phlorotannin’s was limited.

During initial sample preparation (Personal communication), it was also noted that brown and green macroalgal fragments were apparent in the guts of ‘stunted’ *H. iris* at site 2 (Owenga), where the Chlorophytes *Ulva lactuca* and *Codium fragile* were noted to be abundant. It is likely that the green and red alga types are preferable. This selection is

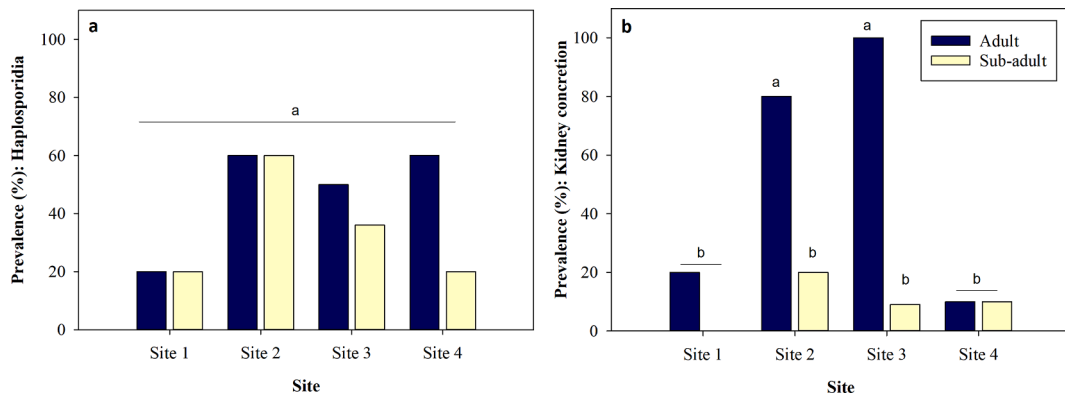


Fig. 10. Population prevalence (%) (n = 10) for the presence/absence of a) haplosporidian-like parasite and b) kidney crystals in the right kidney tissue of *H. iris* from four sites around the Chatham Island (Adults: site 1. Ascots n = 10, site 2. Owenga n = 10, site 3. Durham n = 11, site 4. Wharekauri n = 10; Sub-adults: site 1. Ascots n = 10, site 2. Owenga n = 10, site 3. Durham n = 10, site 4. Wharekauri n = 10). Letters indicate significant differences between sites and life stages ($p < 0.05$).

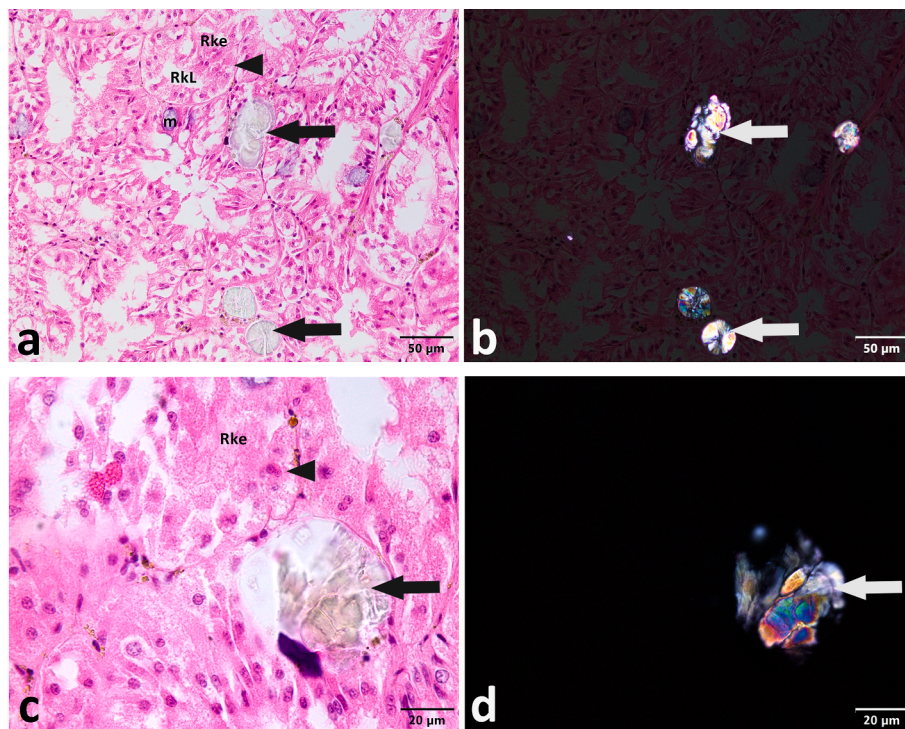


Fig. 11. Crystals in an H&E-stained right kidney section from an adult abalone, viewed under a) bright-field kidney crystals (arrows), b) using a crossed polar filter to observe differences in the inclusions and the anisotropic affect from the birefringent properties c) kidney concretion embedded in the right kidney epithelial (Rke) layer H&E under oil immersion e) oil immersion image of kidney concretion with polarised filter. Right kidney tubule (arrowhead), kidney lumen (RkL), kidney epithelium (Rke) and mucous cells (m).

supported by Foale and Day (1992) and Day and Cook (1995) and whereby it is suggested that NZ abalone have evolved preferences to red and green seaweeds, and only consume phaeophytes when preferred foods are absent. Previous studies investigating the consumption of red and brown seaweeds suggest that soft (non-calcareous) red seaweeds (Rhodophyta) were generally noted to have a higher calorific and nutritional value and often considered to be more attractive and palatable to abalone, subsequently supporting faster growth (Poore, 1973; Britton et al., 2020). It therefore seems reasonable to suggest the availability of Rhodophytes at favourable growth sites, notably Ascots, could substantially explain the improved growth performance of abalone and the greens (e.g., *Ulva* sp.) may not provide the required nutritional components to support faster growth.

U. lactuca was observed to be among the most abundant macrophytes

at three sites (site 1: Ascots, site 2: Owenga and site 3: Durham) with *Durvillea chathamensis* being the most abundant at site 4: Wharekauri. Kelp species such as *D. chathamensis* and *D. antarctica* have been previously described as being the most abundant at the majority of the locations around the Chatham Islands (Schiel, Andrew and Foster, 1995), and Wilcox (2007) gives a general overview of past assemblages. Interestingly, *D. chathamensis* and *Grateloupia prolifera* were previously the most dominant with *U. lactuca* occupying the deeper section of the subtidal zone in Owenga (Wilcox, 2007). This suggests that the assemblage has changed over time, with opportunistic *U. lactuca* replacing the *D. chathamensis* in the upper range and may reflect environmental changes, such as increasing sedimentation (Schiel et al., 2006) and temperature fluctuations (Thomsen et al., 2019). Although the thallus of the *U. lactuca* is soft and palatable to *H. iris*, it is generally regarded as a

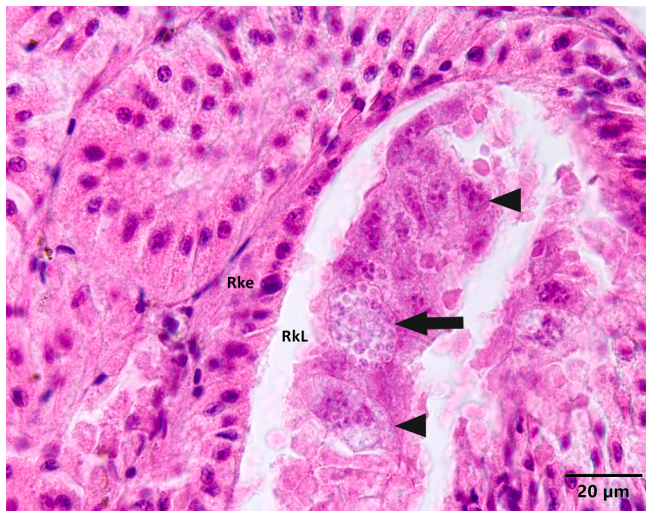


Fig. 12. Multicellular haplosporidian-like parasite (Arrowhead) cluster in the lumen of a right kidney tubule (RkL) of *H. iris*. Right kidney epithelial layer (Rke) and haplosporidian-like sporocyst (arrow).

poor food source as it has a low food conversion ratio and typically results in poor growth rates (Stuart and Brown, 1994). Other sedentary marine invertebrates have been observed to display a high degree of phenotypic plasticity associated with their response to an environmental stressor (Trussell, 1996; Steffani and Branch, 2003; Saunders, Connell and Mayfield, 2009). For example, Saunders, Connell and Mayfield (2009) found that when they translocated *H. rubra* (black-lipped abalone) to a site where the reef topography and algal assemblage supported faster growth, slow-growing, or 'stunted' abalone showed improved compensatory growth rates.

Additionally, the presence of sediment particles found in the gut lumen of the wax-embedded tissue of individual *H. iris* is also of interest. This suggests that *H. iris* are consuming large quantities of sediment when feeding which is likely to have significant nutritional impacts. Ingestion of small amounts of sand and detritus is not uncommon and seen in other abalone species (Harris, Burke and Maguire, 1998). Further analysis of the types of algae that the *H. iris* are consuming as well as the amount of sand compared to the algae ingested would be beneficial and supplementary to the present study. Care also needs to be taken in relation to sample quality and interpretation, with such high levels of sand typically being lost during histological sectioning, leaving voids in the lumen, introducing a risk of misinterpretation of tissues e.g., the intestinal tract.

4.2. Ceroid granules

The accumulation of ceroid material was observed in greater numbers in the connective tissue of the gut, digestive gland, and right kidney in the 'stunted' Owenga *H. iris* population. Ceroid or lipofuscin-like cells are pigmented brown to yellow waxy aggregates formed as a consequence of oxidative stress (Carella, 2015; Webb and Duncan, 2019). Traditionally, lipofuscin accumulation has been associated with age-dependent pigments e.g., in clams (Lomovasky et al., 2002), whereas ceroid pigments have been associated with pathological conditions (Zaroogian and Yevich, 1993; Seehafer and Pearce, 2006; Jung, Bader and Grune, 2007). Pathological conditions include immune response to pathogens (Zaroogian and Yevich, 1993), contaminant degradation and detoxification, e.g. mussels (Carella, 2015; Shaw et al., 2019), and metals accumulation, e.g. oysters (Apeti et al., 2014). Ceroid material has been previously correlated with metals, including cadmium, copper, iron, mercury, and zinc, in mussels, clams and oysters (Thomson, Pirie and George, 1985; Zaroogian and Yevich, 1993; Marigomez et al., 2002).

The proliferation of ceroid observed in the stunted individuals in the present study could be associated with either: an advancement in age (e.g., physiological vs chronological age) (e.g., Basova et al., 2012), as 'stunted' individuals are generally older than their fast-growing neighbours, or the accumulation of metals derived from consumption of contaminated seaweed or sediments, thus presenting in the gut, digestive glands, and right kidney as the sites of absorption and excretion. Conversely, the proliferation could be a result of excessive oxidative stress and disease from pathological conditions associated with sub-optimal conditions and summer marine heatwaves. Additional research is required to elucidate the production and function of the different manifestations of ceroid granules observed and their connection to different processes (Webb and Duncan, 2019). Additionally, further investigation is required to unravel the site-specific influence of aging, pathogens, and environmental perturbations upon ceroid and/or lipofuscin accumulation in abalone and, determine the differences between ceroid and lipofuscin pigments in *H. iris*.

4.3. Kidney crystals

The appearance of crystalline crystals, or 'spherites', similar to human kidney stones, in the right kidney of *H. iris* potentially provides additional clues to environmental perturbations and diet inefficiencies. The prevalence of crystals was high in the adults from the nominally slow-growing sites at Owenga and Durham. The appearance of the crystals was that of a harden and shattered crystalline structure with an anisotropic affect, and therefore referred to here as a 'kidney crystal'. Kidney crystals of different sizes and morphology may occur during environmental stress, resulting from contaminated water, temperature stress, salinity and/or anoxia, such as in the bivalves *Argopecten irradians* and *Mercenaria mercenaria* (Doyle et al., 1978; Carmichael, Squibb and Fowler, 1979; Mauri and Orlando, 1982; Klobucar, Lajtner and Erben, 2001), as well as nutritional and reproductive stress (Klobucar, Lajtner and Erben, 2001). Previously Doyle et al. (1978) note that kidney crystals could develop in various textures and colours, from dark brown and black to ochre and beige, with a diameter of up to 250 μm in *M. mercenaria* and are most commonly associated with phosphorite formation, particularly mineralised magnesium/ calcium Mg/Ca as phosphate and carbonate. Calcium phosphate mineralisation has been observed in kidney of the cephalopod *Nautilus pompilius* and reported as whitlockite uroliths. The uroliths were initially considered as potential storage for Ca ions to be mobilised during septal formation (Crick et al., 2009). There are several examples of the development of crystals in response to toxins, e.g. pentachlorophenol (PCP) in the snail *Planorbis cornus* (Klobucar, Lajtner and Erben, 2001) and cadmium exposure in *A. irradians*, with the possibility that the development is a mechanism for removing excess toxins. However, it should be noted that these were previously described as yellow to brown in colour, in contrast to the clear crystals observed herein (Carmichael, Squibb and Fowler, 1979; Carmichael and Fowler, 1981). Concretion granules of up to 20 μm in diameter have been described in scallops, *Pecten maximus*, with the increase in size thought to reflect the longer residence time in the tissue, (Marigomez et al., 2002).

The kidney crystals found in this study are reminiscent of calcium oxalate crystals found in vertebrate kidney stone disease (nephrolithiasis) with similarities in colour, clarity and texture when stained with H&E and similar anisotropic properties under polarised light (Geraghty, Wood and Sayer, 2020; Nicholas Cossey, Dvanajscak and Larsen, 2020). Possible causes of vertebrate kidney stone disease include hyperoxaluria, high oxalate diets, thiamine/ pyridoxine deficiencies, excessive dieting and alterations in interstitial flora (Geraghty, Wood and Sayer, 2020). Therefore, there is a possibility that the limited food access and ingestion of sediments in the *H. iris* is causing these crystals. Furthermore, calcium carbonate polymorph crystals: calcite, aragonite and vaterite, are common birefringent minerals used in molluscan shell development, the latter associated with shell repair and pearling (Spann,

Harper and Aldridge, 2010; Checa, 2018). There are several potential constituents of such crystals in molluscs including, magnesium oxalate, calcium oxalate and calcium phosphate (the latter as whitlockite, brushite, and hydroxyapatite) (Tiffany, Luer and Watkins, 1980; Crick et al., 2009). In mammal nephrolithiasis calcite and vaterite have been shown to promote calcium oxalate crystallisation (Geider et al., 1996). Further research is required to determine what the composition of the crystals is, as well as the causes and consequences for *H. iris*.

4.4. Pathogen detection

Ectocommensal *Sphenophyra*-like ciliates (Diggles and Oliver, 2005) were recorded in most of the individuals collected. Ciliates are commonly found in close association with many marine molluscs and attachment to the gill filaments is generally superficial (Bower, McGladdery and Price, 1994; Bower, 2006). No signs of effect were evident on the gill epithelium, nor was there evidence of the immunological response or hemocytosis observed in this study as opposed to effected tissues in the geoduck (*Panopea abbreviate*) by Vázquez, Ituarte and Cremonte (2015). It is worth noting that ciliates may become pathological at higher intensities, restricting water flow over the gill filaments and reducing host respiration rates (Vázquez, Ituarte and Cremonte, 2015).

The prevalence of a haplosporidian-like parasite species in the 'stunted' population and could be a contributing factor to the slower host growth. This haplosporidian-like parasite shows similarity to the novel haplosporidian identified by Diggles et al. (2002) and Hine et al. (2002) in farmed *H. iris* in New Zealand during a mortality event in 2000 and 2001. Both Hine et al. (2002) and Diggles et al. (2002) suggested that the appearance of the haplosporidian parasite could be associated with poor growth and condition, although it remains unclear whether the pathogen represents a cause or effect. Diggles et al. (2002) suggested that the appearance of larger parasite cells within the right kidney, when compared with other infected tissues, could potentially be due to low intensity levels and is perhaps representative of natural infection level in wild populations. Haplosporidian parasites are considered to be "of concern" to aquatic animal industries worldwide (Arzul and Carnegie, 2015). The haplosporidian group includes three well-known species that cause epizootic disease in oysters; *Haplosporidium nelsoni*, *Bonamia ostreae* and *Bonamia exitiosa* (Hill et al., 2014; Arzul and Carnegie, 2015; Hine, 2020) and also includes *Urosporidium* sp. (Le et al., 2015) (Arzul and Carnegie, 2015). Very little is known about the haplosporidian species found in *H. iris*, other than the fact that in high levels it can cause mortalities, and DNA sequencing places it close to *Urosporidium* (Reece and Stokes, 2003). Further research is required to robustly identify this haplosporidian – *Urosporidium*, as well as clarifying its current host-interactions, before considering the future implications under the influence of climate change.

4.5. Additional factors and implications

There are two effects yet to be addressed; 1) the sections in some cases displayed minor to moderate distortion, potentially due to sand or sediments in the guts of the abalone and 2) the changes in the digestive tubules, including shrinkage of the epithelial tissue away from the basal membrane, and the compression and increased staining affinity of the basophilic cells. Similar shrinkage and the detachment effect has been indicated previously in the crustacean *Nephrops norvegicus* as a result of starvation (Karapanagiotidis et al., 2015). However, due to the lack of proteinous material in the voids, a fixation affect cannot yet be ruled out (Wolf et al., 2015; Webb, 2020). This effect warrants further investigation to distinguish fixative artefacts from the influence of environmental toxicity and nutrition, as well as establishing why some individuals are more affected by the process than others.

Histopathology is an essential and powerful tool for diagnosing stressors in various environments and providing general assessment of

an individual's health (Hooper et al., 2014; Costa, 2018). It is not without its limitations and misinterpretation can arise from sampling and fixation issues, preparation artefacts and variable observer expertise. Knowledge of the fine-scale changes seen through histological techniques is required to fully understand the effects of a stressor on the individual, particularly the subtle effects of heat, feeding, nutrition and diseases (Hooper et al., 2014). There are very few studies that define a clear baseline range for the variability in tissue structure between individuals under 'real-world' conditions (Costa et al., 2013; Damodaran, 2020); this shortfall should be addressed in future studies.

The designation of the 'stunted' and 'non-stunted' *H. iris* populations was based on both anecdotal observations from the industry experience and descriptions by McShane et al. (1994) and Naylor, Andrew and Kim (2006). The morphometric values such as weight and length broadly supported the 'stunted' vs fast-growing parameters in the adults, however the length to height ratio showed no differences. A larger sample size could have helped to reduce population variability improving the analysis. Nutrition is hypothesised to be the key driver due to direct observation of habitat and seaweed assemblage and is a potential factor for growth performance. It is worth investigating further, not only the analysis of gut contents, but the timing of analysis. Gut contents can be bias towards less digestible alga and timing of analysis is key to correct interpretation due to the ingestion and evacuation rates of food consumption (Foale and Day, 1992; Day and Cook, 1995). There are also additional potential contributing factors that could be driving the divergence in growth performance for example local increases in sedimentation, temperature, and pathogens.

4.6. Conclusions

The histopathological assessment broadly supported the growth performance differences between the 'stunted' and 'non-stunted' populations. The differences in the algal quality, the level of ceroid material found in multiple tissues, the appearance of kidney crystals and the appearance of a haplosporidian-like parasite are potential causative agents of the reduced growth performance. Although the sample size is small in comparison to WOA recommendations (WOAH, 2015), this investigation provided an opportunity to gain valuable insight into the current tissue condition of a small number individual *H. iris* populations around the Chatham Islands. Greater sampling numbers and timepoints will ultimately help elucidate the drivers behind variable growth performance and potential sensitivity to climate change. Not only is further sampling and surveillance required to gain a better understanding, but further research is needed to clarify the causes of the effects identified in this study, especially with regards to the extent to which food availability, digestibility, pathogen loads, and environmental conditions contribute to growth performance of *H. iris*.

Declaration of competing interest

The authors declare that they have no known competing financial interests or personal relationships that could have appeared to influence the work reported in this paper.

Acknowledgement

This research was funded by the New Zealand Ministry for Business, Innovation and Employment, through the Aquaculture Health Strategies to Maximise Productivity and Security programme (CAWX1707) and Cawthron's Shellfish Aquaculture Platform (CAWX1801). We offer special thanks to Nick Cameron (PAUMAC4) and Tom McCowan, Jeremy Cooper (Pāua Industry Council) for their guidance and logistical support. We thank the team at Cawthron and the Aquaculture Biotechnology Research Group, AUT for their intellectual and practical input. We would also like to thank Dr Natali Delorme and Dr Lizenn Delisle for their intellectual support, Paula Casanovas and Martin Cheng for the

assistance with statistical analysis in R, and Medlab Central Histopathology, Palmerston North, and Gribbles veterinary histology department for their assistance with histology processing.

Appendix A. Supplementary data

Supplementary data to this article can be found online at <https://doi.org/10.1016/j.jip.2023.108042>.

References:

- Allen, V.J., Marsden, I.D., Ragg, N.L.C., Gieseg, S., 2006. The effects of tactile stimulants on feeding, growth, behaviour, and meat quality of cultured blackfoot abalone. *Haliotis Iris*. *Aquaculture*. 257, 294–308.
- Apeti, D. A., Lauenstein, G., Warner, R. A., Kim, Y., Tull, J., 2014. Occurrence of Parasites and Diseases in Oysters and Mussels of Us Coastal Waters National Status and Trends, the Mussel Watch Monitoring Program.
- Arzul, L., Carnegie, R.B., 2015. New perspective on the haplosporidian parasites of molluscs. *J Invertebr Pathol*. 131, 32–42.
- Basova, L., Begum, S., Strahl, J., Sukhotin, A., Brey, T., Philipp, E., Abele, D., 2012. Age-dependent patterns of antioxidants in *Arctica Islandica* from six regionally separate populations with different lifespans. *Aquat. Biol.* 14, 141–152.
- Bergström, P., Lindegardh, M., 2016. Environmental influence on mussel (*Mytilus Edulis*) Growth – a quantile regression approach. *Estuar. Coast. Shelf Sci.* 171, 123–132.
- Bower, S.M., 2006. Synopsis of infectious diseases and parasites of commercially exploited shellfish. Ciliates Associated with Abalone. Dfo.
- Bower, S.M., McGladdery, S.E., Price, I.M., 1994. Synopsis of infectious diseases and parasites of commercially exploited shellfish. *Sphenophrya*-like Ciliates of Clams and Cockles. Dfo.
- Britton, D., Schmid, M., Revill, A.T., Virtue, P., Nichols, P.D., Hurd, C.L., Mundy, C.N., 2020. Seasonal and site-specific variation in the nutritional quality of temperate seaweed assemblages: implications for grazing invertebrates and the commercial exploitation of seaweeds. *J. Appl. Phycol.* 33, 603–616.
- Britz, P.J., Hecht, T., Knauer, J., 1996. Gastric evacuation time and digestive enzyme activity in abalone *Haliotis Midae* fed a formulated diet. *S. Afr. J. Mar. Sci.* 17, 297–303.
- Carella, F.F., Bignell, S.W., DeVico, J.P., G., 2015. Comparative pathology in bivalves: etiological agents and disease processes. *J. Invertebr. Pathol.* 131, 13.
- Carmichael, N.G., Fowler, B.A., 1981. Cadmium accumulation and toxicity in the kidney of the bay scallop *Argopecten Irradians*. *Mar. Biol.* 65, 35–43.
- Carmichael, N.G., Squibb, K.S., Fowler, B.A., 1979. Metals in the molluscan kidney: a comparison of two closely related bivalve species (*Argopecten*), Using X-Ray microanalysis and atomic absorption spectroscopy. *J. Fish. Res. Board Can.* 36, 1149–1155.
- Checa, A.G., 2018. Physical and biological determinants of the fabrication of molluscan shell microstructures. *frontiers in marine science*. Science 5.
- Costa, P.M., 2018. Introduction. In: Costa, P.M. (Ed.), *The Handbook of Histopathological Practices in Aquatic Environments*. Academic Press, pp. 1–20.
- Costa, P.M., Carreira, S., Costa, M.H., Caeiro, S., 2013. Development of histopathological indices in a commercial marine bivalve (*Ruditapes Decussatus*) to determine environmental quality. *Aquat Toxicol.* 126, 442–454.
- Crick, R.E., Burkart, B., Chamberlain, J.A., Mann, K.O., 2009. Chemistry of calcified portions of *Nautilus Pompilius*. *J. Mar. Biol. Assoc. U. K.* 65, 415–420.
- Cuevas, N., Zorita, I., Costa, P.M., Franco, J., Larreta, J., 2015. Development of histopathological indices in the digestive gland and gonad of mussels: integration with contamination levels and effects of confounding factors. *Aquat. Toxicol.* 162, 152–164.
- Cule, E. S., Frankowski, M. D., Ridge: Ridge Regression with Automatic Selection of the Penalty Parameter. R package version 3.0, <https://CRAN.R-project.org/package=ridge>, 2021.
- Damodaran, D., Morphological. 2020. Histological and behavioural change in two species of marine bivalves in response to environmental stress. *Marine Biology*, Vol. Masters. Victoria University of Wellington 130.
- Day, R.W., Cook, P., 1995. Bias Towards Brown Algae in Determining Diet and Food Preferences: the South African Abalone *Haliotis Midae*. *Mar. Freshw. Res.* 46, 623–627.
- Diggles, B.K., Nichol, J., Hin, P.M., Wakefield, S., Cochenec-Laureau, N., Roberts, R.D., Friedman, C.S., 2002. Pathology of Cultured Paua *Haliotis Iris* Infected with a Novel Haplosporidian Parasite, with some observations on the course of disease. *Dis. Aquat. Organ.* 50, 219–231.
- Diggles, B.K., Oliver, M., 2005. Diseases of cultured paua (*Haliotis Iris*) in New Zealand. *Diseases in Asian Aquaculture* 275–287.
- Doyle, L.J., Blake, N.J., Woo, C.C., Yevich, P., 1978. Recent biogenic phosphorite: concretions in mollusk kidneys. *Science* 199, 1431–1433.
- Foale, S., Day, R., 1992. Recognizability of algae ingested by abalone. *Mar. Freshw. Res.* 43, 1331–1338.
- Fraga, N., Benito, D., Briaudeau, T., Izagirre, U., Ruiz, P., 2022. Toxicopathic effects of lithium in mussels. *Chemosphere* 307, 136022.
- Geider, S., Dussol, B., Nitsche, S., Veesler, S., Berthezene, P., Dupuy, P., Astier, J.P., Boistelle, R., Berland, Y., Dagorn, J.C., Verdier, J.M., 1996. Calcium carbonate crystals promote calcium oxalate crystallization by heterogeneous or epitaxial nucleation: possible involvement in the control of urinary lithogenesis. *Calcif. Tissue Int.* 59, 33–37.
- Geraghty, R., Wood, K., Sayer, J.A., 2020. Calcium oxalate crystal deposition in the kidney: identification, causes and consequences. *Urolithiasis*. 48, 377–384.
- Halpern, B.S., Walbridge, S., Selkoe, K.A., Kappel, C.V., Micheli, F., D'Agrosa, C., Bruno, J.F., Casey, K.S., Ebert, C., Fox, H.E., Fujita, R., Heinemann, D., Lenihan, H.S., Madin, E.M., Perry, M.T., Selig, E.R., Spalding, M., Steneck, R., Watson, R., 2008. A global map of human impact on marine ecosystems. *Science* 319, 948–952.
- Harris, J., Burke, C., Maguire, G., 1998. Characterisation of the digestive tract of greenlip abalone, *Haliotis Laevigata* donovan. i. morphology and histology. *J. Shellfish. Res.* 17, 979–988.
- Hill, K.M., Stokes, N.A., Webb, S.C., Hine, P.M., Kroeck, M.A., Moore, J.D., Morley, M.S., Reece, K.S., Bureson, E.M., Carnegie, R.B., 2014. Phylogenetics of bonamia parasites based on small subunit and internal transcribed spacer region ribosomal DNA sequence data. *Dis. Aquat. Organ.* 110, 33–54.
- Hine, P.M., 1997. Health Status of Commercially Important Molluscs in New Zealand. Ministry for Primary Industries.
- Hine, P.M., 2020. Haplosporidian host: parasite interactions. *Fish Shellfish Immunol.* 103, 190–199.
- Hine, P.M., Wakefield, S., Diggles, B.K., Webb, V.L., Maas, E.W., 2002. Ultrastructure of a haplosporidian containing rickettsiae, associated with mortalities among cultured Paua *Haliotis Iris*. *Dis. Aquat. Organ.* 49, 207–219.
- Hooper, C., Day, R., Slocombe, R., Benkendorff, K., Handlinger, J., Goulias, J., 2014. Effects of severe heat stress on immune function, biochemistry and histopathology in farmed Australian Abalone (Hybrid *Haliotis Laevigata* × *Haliotis Rubra*). *Aquaculture* 432, 26–37.
- Howard, D. W., 2004. *Histological Techniques for Marine Bivalve Mollusks and Crustaceans*. NOAA, National Ocean Service, National Centers for Coastal Ocean Service, Center for Coastal Environmental Health and Biomolecular Research, Cooperative Oxford Laboratory.
- Jung, T., Bader, N., Grune, T., 2007. Lipofuscin: formation, distribution, and metabolic consequences. *Ann N Y Acad Sci.* 1119, 97–111.
- Kang, D.-H., Chu, F.-L.-E., Yang, H.-S., Lee, C.-H., Koh, H.-B., Choi, K.-S., 2010. Growth, reproductive condition, and digestive tubule atrophy of pacific oyster *Crassostrea Gigas* in Gamakman Bay Off the Southern Coast of Korea. *J. Shellfish. Res.* 29, 839–845.
- Karapanagiotidis, I.T., Mente, E., Berillis, P., Rotllant, G., 2015. Measurement of the feed consumption of *Nephtys Norvegicus* feeding on different diets and its effect on body nutrient composition and digestive gland histology. *J. Crustac. Biol.* 35, 11–19.
- Klobucar, G.I., Lajtner, J., Erben, R., 2001. Increase in number and size of kidney concretions as a result of pcp exposure in the freshwater snail *Planorbis Corneus* (Gastropoda, Pulmonata). *Dis. Aquat. Organ.* 44, 149–154.
- Knowles, G., Handlinger, J., Jones, B., Moltschanivskiy, N., 2014. Hemolymph chemistry and histopathological changes in pacific oysters (*Crassostrea Gigas*) in response to low salinity stress. *J. Invertebr Pathol.* 121, 78–84.
- Laferriere, A.A.M., 2016. Examining the Ecological Complexities of Blackfoot Paua Demography and Habitat Requirements in the Scope of Marine Reserve Protection, Vol. Doctorate. Victoria University of Wellington, Victoria University of Wellington.
- Le, T.C., Kang, H.S., Hong, H.K., Park, K.J., Choi, K.S., 2015. First Report of Urosporidium Sp., a Haplosporidian Hyperparasite Infecting Digenean Trematode *Parvatrema Duboisii* in Manila Clam, *Ruditapes Philippinarum* on the West Coast of Korea. *J. Invertebr Pathol.* 130, 141–146.
- Lenth, R. V., *Emmeans: Estimated Marginal Means, Aka Least-Squares Means*. R package version 1.7.1-1, <https://CRAN.R-project.org/package=emmeans>, 2021.
- Lima, F.P., Wetthey, D.S., 2012. Three decades of high-resolution coastal sea surface temperatures reveal more than warming. *Nat Commun.* 3, 704.
- Lomovasky, B.J., Morriconi, E., Brey, T., Calvo, J., 2002. Individual age and connective tissue lipofuscin in the hard clam *Eurhomalea Exalbida*. *J. Exp. Mar. Biol. Ecol.* 276, 83–94.
- Mai, K., Mercer, J.P., Donlon, J., 1995. Comparative studies on the nutrition of two species of abalone, *Haliotis Tuberculata* L. And *Haliotis Discus Hannai* Ino. iii. response of abalone to various levels of dietary lipid. *Aquaculture* 134, 65–80.
- Marigomez, I., Soto, M., Cajaraville, M.P., Angulo, E., Giamberini, L., 2002. Cellular and subcellular distribution of metals in molluscs. *Microsc Res Tech.* 56, 358–392.
- Martin, R.J., Bergey, E.A., 2013. Growth plasticity with changing diet in the land snail *Patera Appressa* (Polygyridae). *J. Moll. Stud.* 79, 364–368.
- Mauri, M., Orlando, E., 1982. Experimental Study on renal concretions in the wedge shell *Donax Trunculus* L. *J. Exp. Mar. Biol. Ecol.* 63, 47–57.
- McShane, P.E., Naylor, J.R., 1995. Small-Scale Spatial Variation in Growth, Size at Maturity, and Yield- and Egg-Per-Recruit Relations in the New Zealand Abalone *Haliotis Iris*. *N. Z. J. Mar. Freshw. Res.* 29, 603–612.
- McShane, P.E., Schiel, D.R., Mercer, S.F., Murray, T., 1994. Morphometric variation in *Haliotis Iris* (Mollusca: Gastropoda): analysis of 61 populations. *N. Z. J. Mar. Freshw. Res.* 28, 357–364.
- Morash, A.J., Alter, K., 2016. Effects of environmental and farm stress on abalone physiology: perspectives for abalone aquaculture in the face of global climate change. *Rev. Aquac.* 8, 342–368.
- Muznebin, F., Alfaro, A.C., Webb, S.C., 2021. Occurrence of *Perkinsus Olseni* and other parasites in New Zealand Black-footed Abalone (*Haliotis Iris*). *N. Z. J. Mar. Freshw. Res.* 57, 261–281.
- Muznebin, F., Alfaro, A.C., Webb, S.C., 2022. *Perkinsus Olseni* and other parasites and abnormal tissue structures in New Zealand Greenshell™ Mussels (*Perna Canaliculus*) across different seasons. *Aquac. Int.* 31, 547–582.
- Naylor, J.R., Andrew, N., 2004. Productivity and Response to Fishing of Stunted Paua Stocks. Ministry of Fisheries.
- Naylor, J.R., Andrew, N.L., Kim, S.W., 2006. Demographic Variation in the New Zealand Abalone *Haliotis Iris*. *Mar. Freshw. Res.* 57, 215–224.

- Naylor, J.R., Manighetti, B.M., Neil, H.L., Kim, S.W., 2007. Validated estimation of growth and age in the New Zealand abalone *Haliotis Iris* using stable oxygen isotopes. *Mar. Freshw. Res.* 58, 354–362.
- Nicholas Cossey, L., Dvanajscak, Z., Larsen, C.P., 2020. A Diagnostician's field guide to crystalline nephropathies. *Semin Diagn Pathol.* 37, 135–142.
- Pérez-Cebreco, M., Prieto, D., Blanco-Rayón, E., Izagirre, U., Ibarrola, I., 2022. Differential tissue development compromising the growth rate and physiological performances of mussel. *Marine Environmental Research* 180, 105725.
- Poore, G.C.B., 1972. Ecology of New Zealand Abalones, *Haliotis* species (Mollusca: Gastropoda). *N. Z. J. Mar. Freshw. Res.* 6, 11–22.
- Poore, G.C.B., 1973. Ecology of New Zealand abalones, *Haliotis* species (Mollusca: Gastropoda). *N. Z. J. Mar. Freshw. Res.* 7, 67–84.
- R Core Team, R: A Language and Environment for Statistical Computing. R Foundation for Statistical Computing. Vienna, Austria, <https://www.R-project.org/>, 2021.
- Reece, K.S., Stokes, N.A., 2003. Molecular analysis of a haplosporidian parasite from cultured new zealand abalone *Haliotis Iris*. *Dis. Aquat. Organ.* 53, 61–66.
- Ren, J.S., Fox, S.P., Howard-Williams, C., Zhang, J., Schiel, D.R., 2019. Effects of stock origin and environment on growth and reproduction of the green-lipped mussel *Perna Canaliculus*. *Aquaculture* 505, 502–509.
- Saulsbury, J., Moss, D.K., Ivany, L.C., Kowalewski, M., Lindberg, D.R., Gillooly, J.F., Heim, N.A., McClain, C.R., Payne, J.L., Roopnarine, P.D., Schöne, B.R., Goodwin, D., Finnegan, S., 2019. Evaluating the influences of temperature, primary production, and evolutionary history on bivalve growth rates. *Paleobiology* 45, 405–420.
- Saunders, T.M., Mayfield, S., Hogg, A.A., 2008. A simple, cost-effective, morphometric marker for characterising abalone populations at multiple spatial scales. *Mar. Freshw. Res.* 59, 32–40.
- Saunders, T.M., Connell, S.D., Mayfield, S., 2009b. Differences in abalone growth and morphology between locations with high and low food availability: morphologically fixed or plastic traits? *Mar. Biol.* 156, 1255–1263.
- Saunders, T., Mayfield, S., Hogg, A., 2009a. Using a simple morphometric marker to identify spatial units for abalone fishery management. *ICES J. Mar. Sci.* 66, 305–314.
- Schiel, D.R., Andrew, N.L., Foster, M.S., 1995. The structure of subtidal algal and invertebrate assemblages at the Chatham Islands. *New Zealand. Marine Biology.* 123, 355–367.
- Schiel, D.R., Wood, S.A., Dunmore, R.A., Taylor, D.I., 2006. Sediment on rocky intertidal reefs: effects on early post-settlement stages of habitat-forming seaweeds. *J. Exp. Mar. Biol. Ecol.* 331, 158–172.
- Searle, T., Roberts, R.D., Lokman, P.M., 2006. Effects of temperature on growth of juvenile blackfoot abalone. *Haliotis Iris* Gmelin. *Aquaculture Research.* 37, 1441–1449.
- Seehafer, S.S., Pearce, D.A., 2006. You say lipofuscin, we say ceroid: defining autofluorescent storage material. *Neurobiol Aging.* 27, 576–588.
- Shaw, J.P., Moore, M.N., Readman, J.W., Mou, Z., Langston, W.J., Lowe, D.M., Frickers, P.E., Al-Moosawi, L., Pascoe, C., Beesley, A., 2019. Oxidative stress, lysosomal damage and dysfunctional autophagy in molluscan hepatopancreas (Digestive Gland) induced by chemical contaminants. *Mar. Environ. Res.* 152, 104825.
- Shumway, S.E., Parsons, G.J., 2011. *Scallops: Biology*. Elsevier, Ecology and Aquaculture.
- Soon, T.K., Ransangan, J., 2019. Extrinsic factors and marine bivalve mass mortalities: an overview. *J. Shellfish. Res.* 38 (223–232), 10.
- Spann, N., Harper, E.M., Aldridge, D.C., 2010. The unusual mineral vaterite in shells of the freshwater Bivalve *Corbicula Fluminea* from the UK. *Naturwissenschaften* 97, 743–751.
- Steffani, C.N., Branch, G.M., 2003. Growth rate, condition, and shell shape of *Mytilus Galloprovincialis*: responses to wave exposure. *Mar. Ecol. Prog. Ser.* 246, 197–209.
- Stuart, M.D., Brown, M.T., 1994. Growth and diet of cultivated black-footed abalone, *Haliotis Iris* (Martyn). *Aquaculture* 127, 329–337.
- Thomsen, M.S., Mondardini, L., Alestra, T., Gerrity, S., Tait, L., South, P.M., Lilley, S.A., Schiel, D.R., 2019. Local extinction of bull kelp (*Durvillaea* Spp.) due to a marine heatwave. *frontiers in marine. Science* 6.
- Thomson, J.D., Pirie, B.J., George, S.G., 1985. Cellular metal distribution in the pacific oyster, *Crassostrea Gigas* (Thun.) determined by quantitative X-Ray microprobe analysis. *J. Exp. Mar. Biol. Ecol.* 85, 37–45.
- Tiffany 3rd, W.J., Luer, W.H., Watkins, M.A., 1980. Intracellular and intraluminal aspects of renal calculosis in the marine mollusc *Macrocallysta Nimbosa*. *Invest. Urol.* 18, 139–143.
- Trussell, G.C., 1996. Phenotypic plasticity in an intertidal snail: the role of a common crab predator. *Evolution* 50, 448–454.
- Vázquez, N., Ituarte, C., Cremonte, F., 2015. A Histopathological Study of the Geoduck Clam *Panopea Abbreviata* from San José Gulf, North Patagonia, Argentina. *J. Mar. Biol. Assoc. U. K.* 95, 1173–1181.
- Venables, B., Ripley, B., *Modern Applied Statistics with S*. 2002.
- Viera, M.P., de Vicoso, G.C., Gómez-Pinchetti, J.L., Bilbao, A., Fernandez-Palacios, H., Izquierdo, M.S., 2011. Comparative performances of juvenile abalone (*Haliotis Tuberculata Coccinea* Reeve) fed enriched Vs non-enriched macroalgae: effect on growth and body composition. *Aquaculture* 319, 423–429.
- Webb, S.C., Duncan, J., 2019. New Zealand Shellfish Health Monitoring 2007 to 2017: Insights and Projections. *Cawthron Report No. 2568*, 67.
- Webb, S. C., 2020. *Fixative Artefacts in Histology: Mitigation and Interpretation*. *Cawthron Report No. 3502*. 37.
- Wells, F.E., Mulvay, P., 1995. Good and bad fishing areas for *Haliotis Laevigata*: a comparison of population parameters. *Mar. Freshw. Res.* 46, 591–598.
- Wilcox, M.D., 2007. Observations on seaweeds at the chatham Islands. *Auckland Botanical Society Journal.* 61, 27–28.
- WOAH, 2015. Chapter 1.4. *Oie Aquatic Animal Health Surveillance*. *Aquatic Animal Health Code*. <http>.
- Wolf, J.C., Wolfe, M.J., Baumgartner, W.A., Blazer, V.S., Camus, A.C., Engelhardt, J.A., Fournie, J.W., Frasca, S., Groman, D.B., Kent, M.L., Khoo, L.H., Law, J.M., Lombardini, E.D., Ruehl-Fehlert, C., Segner, H.E., Smith, S.A., Spitsbergen, J.M., Weber, K., 2015. Nonlesions, misdiagnoses, missed diagnoses, and other interpretive challenges in fish histopathology studies: a guide for investigators, authors, reviewers, and readers. *Toxicol. Pathol.* 43, 297.
- Wu, Y., Kaiser, H., Jones, C.L.W., 2018. A first study on the effect of dietary soya levels and crystalline isoflavones on growth, gonad development and gonad histology of farmed abalone. *Haliotis Midae*. *Aquaculture International.* 27, 167–193.
- Zarogian, G., Yevich, P., 1993. Cytology and biochemistry of brown cells in *Crassostrea Virginica* collected at clean and contaminated stations. *Environ. Pollut.* 79, 191–197.